Solid Freeform Fabrication 2021: Proceedings of the 32nd Annual International
Solid Freeform Fabrication Symposium – An Additive Manufacturing Conference

Simulation of the Laser-Powder Bed Fusion Process for Determining the Effects of Part-to-Substrate Location and Orientation on Distortion in a Connecting Rod

Benjamin Weinhold[1], Blake Heck[1], Ashton Albright[1], Keran Wang[1], Jon-Michael Grote[1], Emmanuel Adeniji[1], Dr. Mohammad Masoomi[2], Dr. Scott Thompson[1,*]

[1] Alan Levin Department of Mechanical and Nuclear Engineering, Kansas State University, Manhattan, KS 66506

[2] ANSYS Inc., Canonsburg, PA 15317

*Corresponding author: smthompson@ksu.edu

Abstract

The use of process simulation for designing parts and ensuring their effective additive manufacture can result in reduced product development times which would otherwise require costly trial-and-error manufacturing and testing experiments. The goal of this project was to determine the effects of part-to-substrate location and part build orientation on final part quality as measured via distortion. A connecting rod from an engine was selected for re-design for mass reduction and additive manufacturing via laser powder bed fusion (L-PBF). The rod was modeled and optimized using the topology optimization features of ANSYS® Workbench. A mass reduction of ~44% was achieved and unique design features were revealed. After topology optimization, the L-PBF process was simulated using the ANSYS Workbench Additive Wizard while having the optimized rod in three separate orientations at two different substrate locations. In all cases investigated, build orientation proved to have a more significant impact on distortion than substrate location. The effect of over supporting the part for distortion control can be investigated further to circumvent location/orientation dependencies.

Introduction

The additive manufacturing (AM) of complex, low production, high-value metal components is a major growth area in a variety of industries from defense to biomedical [1]. However, there are still several issues with the process which can present problems for parts which require a high degree of precision. Print porosity, deformation, and crack formation can all lead to part failure, sometimes catastrophically [2-3]. As such, computer simulation of the AM process is essential for ensuring good part quality. Otherwise, physical testing would have to be done for every part, resulting in a significant loss of time and productivity for any industry attempting to undertake a move into metal AM. This focus on AM has produced a particular interest in printed part deformation at different locations on the substrate – particularly for the laser powder bed fusion (L-PBF) AM process. This current study examines this issue by utilizing the ANSYS® Topology Optimization module to generate a sufficiently complex part for simulation by optimizing an existing connecting rod from a 6 hp engine. The design was then tested in six finite element analysis (FEA) simulations at two locations using the Additive Wizard extension for ANSYS® Workbench 2020 R2. The conclusions reached were based on the comparison of the distortions at these two locations after the simulated print.

Method

To showcase possible distortion due to orientation and substrate location effects, a baseline part was selected to run optimization on and then measure distortion. A 7075-T651 aluminum connecting rod out of a 4-stroke motor (Predator 212 cc OHV Engine) was selected as shown in Fig. 1. This option was selected due to its accessibility and low cost. There is also potential for such a part to be additive manufactured for mass reduction and optimization. The engine was disassembled, and the connecting rod removed for reverse engineering and measurements.

Figure 1: Disassembled Predator 212 cc OHV engine (left) and connecting rod (right).

A static load case was needed to perform a meaningful topology optimization. A worst case TDC (top dead center) pressure in the range of 2.07 MPa (300 psi) was assumed. Using the bore, displacement, and compression ratio, the axial pressure on the connecting rod at any crank angle can be assumed. The engine specifications are summarized in Table 1.

Table 1. Specifications of Predator 212 cc OHV engine.

Displacement	212 cc
Bore	70 mm
Compression ratio	8.5:1
Connecting Rod Length	84 mm

Equations (1)-(2) were used to estimate the static load on the connecting rod, i.e.:

$$\mathrm{A_{PistonHead}} = \frac{\pi d^2}{4} = \frac{\pi(70)^2}{4} = 3848.45\ \mathrm{mm}^2 = 0.00385\ \mathrm{m}^2 \qquad (1)$$

$$\mathrm{Force_{A,TDC}} = \mathrm{Pressure} \cdot \mathrm{Area_{PistonHead}} = 2.07\ \mathrm{Pa} \cdot 0.00385\ \mathrm{m}^2 \cong 7966.3\ \mathrm{N} \qquad (2)$$

The crank angle was extrapolated using the displacement and compression ratio in Table 1. Figure 1 shows that the loading does not increase on the connecting rod after TDC, thus a loading case of 8000 N is adequate.

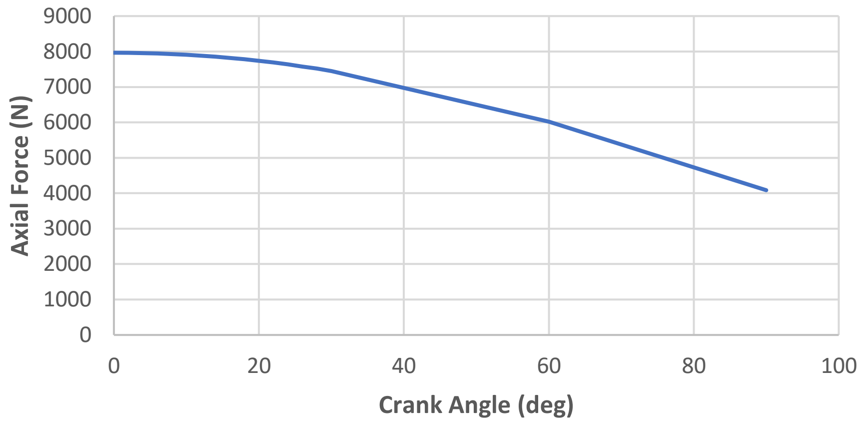

Figure 2: Axial force versus crank angle.

For the topology optimization, a simplified version of the connecting rod base geometry was imported into ANSYS with additional volume in comparison to the original. This additional volume allowed the software to have more material to operate with. The static structure was then evaluated in ANSYS under the static loading scenario discussed above.

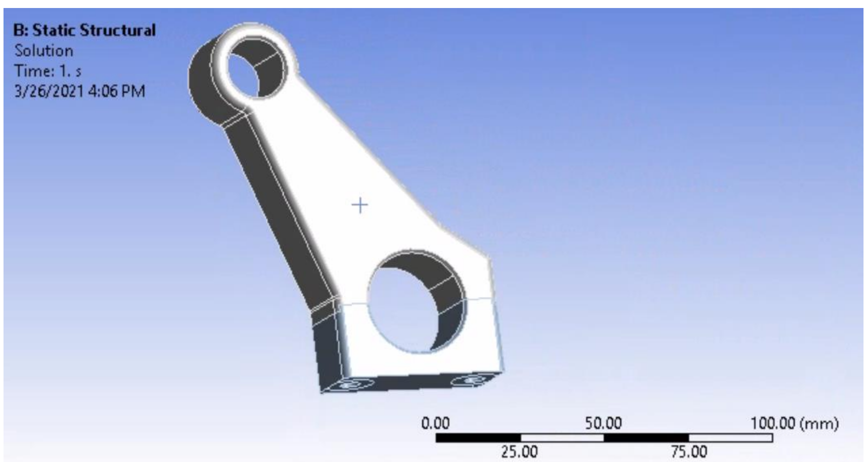

Figure 3: Simplified 3D model of connecting rod for optimization.

Running the topology optimization study with a fine 1-mm linear mesh, from an initial mass of 142.5 grams, a mass reduction of 79.1 grams was achieved. The software workflow is shown in Fig. 4. The final, optimized connecting rod is shown in Fig. 5. Note the multiple spines and curved features in the new connecting rod making it a much stronger candidate for AM.

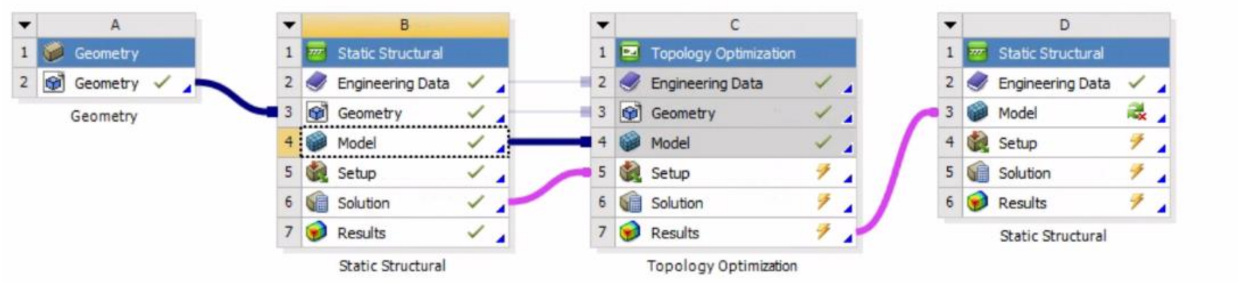

Figure 4: ANSYS workbench optimization workflow.

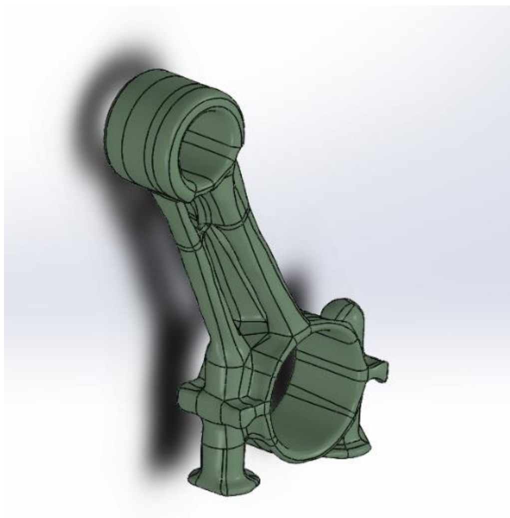

Figure 5: Optimized connecting rod.

The optimized connecting rod was then exported to the AM simulation tool, Additive Wizard, with workflow shown in Fig. 6. The goal was to understand the effects of baseplate location and build orientation on final part deformation – a task well suited for this design-for-AM simulation tool. Six simulations were performed by varying the connecting rod build orientation, at values of 0° (horizontal), 45° (diagonal) and 90° (vertical), and build location on the substrate, being either at the center or corner location. Supports for all connecting rod configurations were automatically generated. The connecting rod material was inputted as AlSi10Mg (cast aluminum) as this is a widely available material with known process parameters for L-PBF.

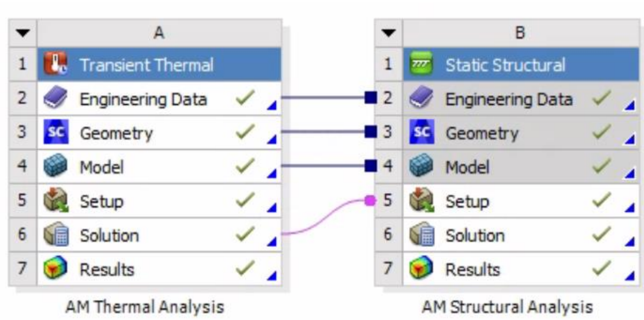

Figure 6: ANSYS Additive Wizard workflow.

Results and Discussion

Results are presented in the form of screenshots that show the distortion contour plots along the connecting rod. Note that contours range from dark blue to red with blue representing small distortion and red representing the larger distortion. Figure 7 shows the distortion of the connecting rod oriented vertically at the corner and corner of the substrate.

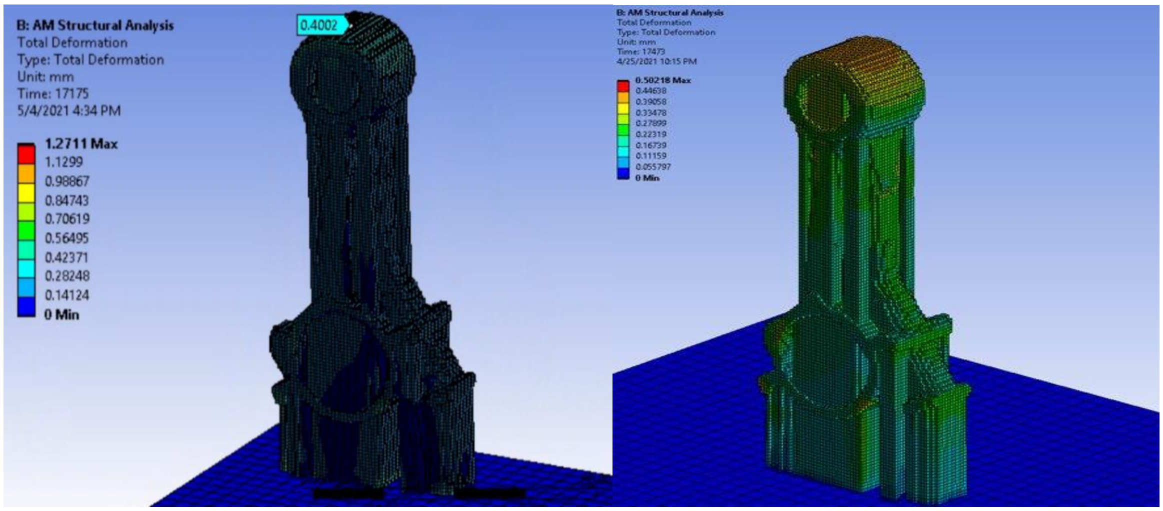

Figure 7: Total deformation contour plots on vertically-oriented (90º) connecting rod (left) at corner and (right) center of substrate.

As shown in Fig. 7, the build location on the substrate impacts connecting rod distortion. The corner location provides for a larger range of distortions whereas the center location has a more even distribution of distortions. Note that the maximum distortion for the corner-located rod (~1.1 mm) skewed the distribution due to contact idiosyncrasy with the substrate which is a known issue in the simulation. Hence, the flagged measurement in Fig. 7 provides a representative deformation at the top surface. The center-located rod had ~10-20% higher distortion along its top surface relative to the corner-located rod. Figure 8 shows the distortion of the connecting rod oriented diagonally at the corner and center of the substrate.

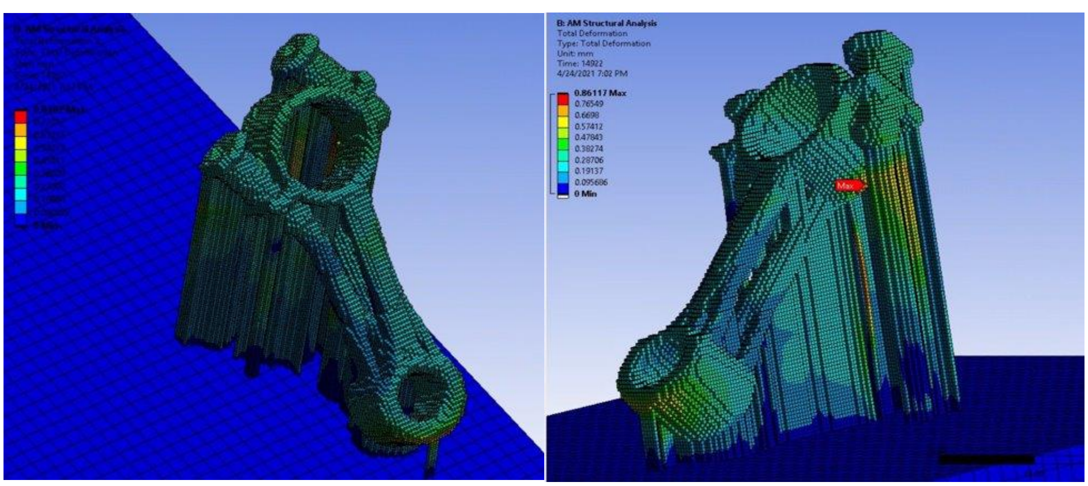

Figure 8: Total deformation contour plots on diagonally-oriented (45º) connecting rod (left) at corner and (right) center of substrate.

The distortion values and range of the connecting rod while in the diagonal orientation are unique relative to the other investigated orientations due to the amount/volume of support structure needing to be more. In 45º orientation, both base plate locations provide for more evenly distributed distortion values. A maximum deformation around 0.8 mm exists for the center-located rod with most of the elevated distortion being in the top regions of the support structures. Figure 9 shows the distortion of the connecting rod oriented horizontally at the corner and center of the substrate.

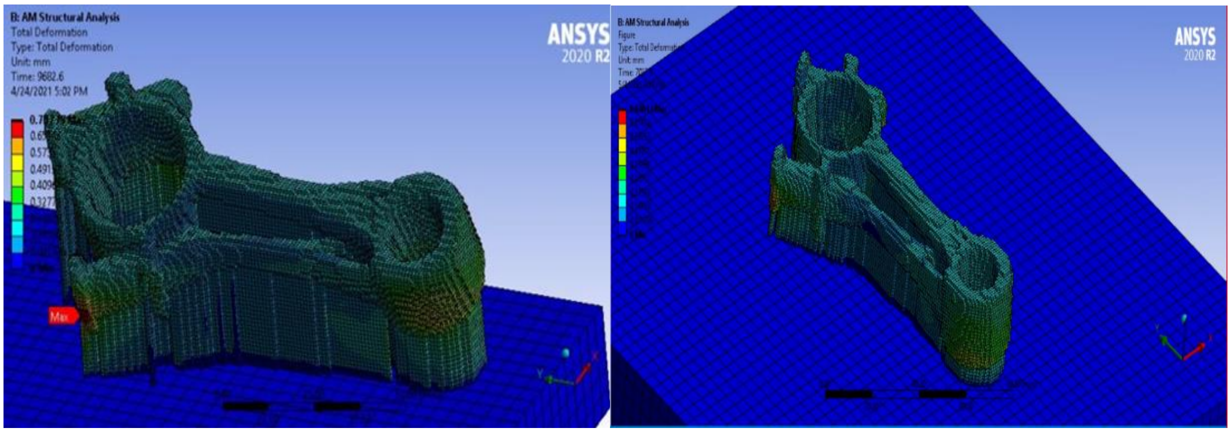

Figure 9: Total deformation contour plots on horizontally-oriented (0º) connecting rod (left) at corner and (right) center of substrate.

The behavior of the 0^0 orientation simulations was comparable to the behavior of the 45^0 orientations. Their distortion was evenly distributed throughout the body. The center location provide for a distortion of 0.17 mm at the top surface of the part and the corner-located configuration provided for a distortion of 0.22 mm.

After running each simulation, the total distortion at the top of each part was found, as shown in Fig. 10. These total deformations were found by extracting individual distortion values from several points along the highest surface of the connecting rod for each simulation. This provided for less-biased distortion measurements for each part. From the results it may be seen that the center-located, horizontally-oriented rod was the most optimal orientation if only distortion is being considered, while the center-located, vertically-oriented rod was least optimal in terms of distortion. Printing the part at the center and at 0^0 resulted in a distortion of 0.17 mm while printing the part at the center and at 90^0 resulted in a distortion of 0.43 mm. There is a 153% increase in distortion when printing the part in the least optimal orientation as opposed to printing in the most optimal orientation. The increase in distortion based on substrate location ranged from 6.3% to 29.4%. On the other hand, changing orientation resulted in a 25% -100 % increase in distortion. This huge disparity supports the argument that part orientation has a more significant impact on distortion than substrate location. Results show that distortion increases with build angle, and this indicates that the per-layer fusion zone may play a role. For example, the horizontally-oriented rod has a much higher area along the build plane (i.e. looking down on the part, aerial view) relative to the vertical rod. This impacts the process heat transfer and residual stress formation.

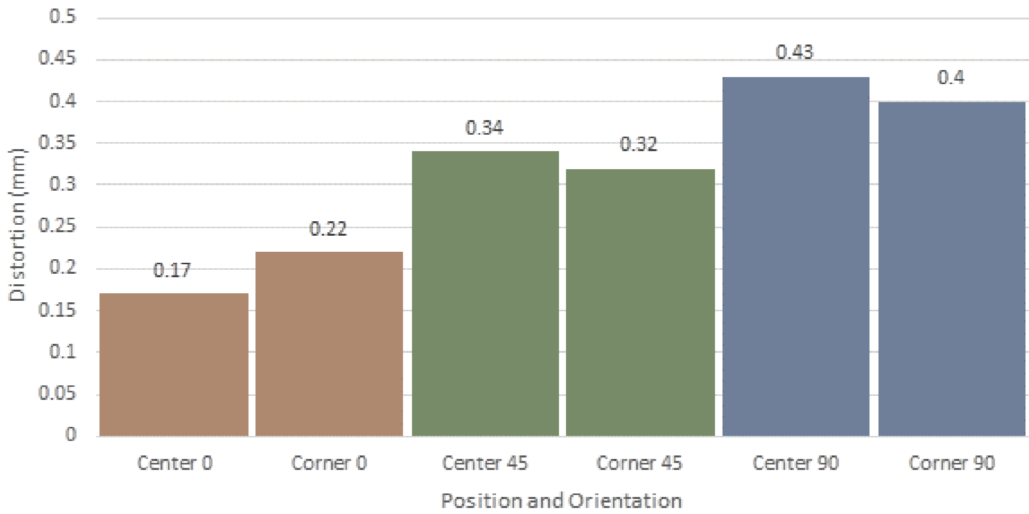

Figure 10: Distortion at the top of connecting rod for the various configurations investigated. Note that 'Center 0' means center location, 0º build orientation.

Conclusions

The L-PBF simulations performed herein via ANSYS® on a topology-optimized AlSi10Mg connecting rod suggest that part orientation has a more significant impact on distortion than base plate location. There were minor differences for a part with the same orientation located at either the center or corner of the substrate. In contrast, a much larger disparity in distortion for different part orientations was observed. Higher build angles generally resulted in higher maximum deformation along the top surface of the connecting rod. The topology realized via a static load boundary constraint resulted in significant mass reduction and a truly unique connecting rod design. The optimized connecting rod is a very suitable candidate for L-PBF, and the simulations are warranted for ensuring part integrity and quality.

Future efforts should include more simulation parameter variations (more angles, locations) as the sample size for the current study was somewhat small. Effects of local heat transfer coefficients related to the purge gas flow in L-PBF should be considered to characterize substrate location effects more accurately. Simulations should be performed on a high-performance computer so that mesh sizes can be reduced for more accurate stress and strain predictions.

References

[2] C. Y. Yap, C. K. Chua, Z. L. Dong, Z. H. Liu, D. Q. Zhang, L. E. Loh, S. L. Sing, "Review of selective laser melting: Materials and applications," Applied Physics Reviews, Vol. 2 (3), 041101 (2015).

[3] A.A. Martin, N.P. Calta, S.A. Khairallah, et al., "Dynamics of pore formation during laser powder bed fusion additive manufacturing," Nature Communications, Vol. 10, Article No. 1987 (2019).

[4] J. Allison, C. Sharpe and C. Seepersad, "Powder bed fusion metrology for additive manufacturing design guidance," Additive Manufacturing, Vol. 25, pp. 239-251 (2019).